

Received December 25, 2019, accepted January 15, 2020, date of publication January 20, 2020, date of current version January 28, 2020.

Digital Object Identifier 10.1109/ACCESS.2020.2967769

Design of Dual-/Wide-Band Quasi-Yagi Antenna Based on a Dielectric Resonator

ZHONG-YU QIAN¹, LING-LING YANG¹, AND JIAN-XIN CHEN^{1,2}, (Senior Member, IEEE)

¹School of Information Science and Technology, Nantong University, Seyuan Road, Nantong 226019, China

²Nantong Research Institute for Advanced Communication Technologies, Nantong 226019, China

Corresponding author: Jian-xin Chen (jjxchen@hotmail.com)

This work was supported in part by the Natural Science Foundation of Jiangsu Province under Grant BK20161281, and in part by the Science-Technology Programs of Nantong under Grant MS12018004.

ABSTRACT This paper presents a design approach of dual-/wide-band quasi-Yagi antenna using a dielectric resonator (DR). A single rectangular DR operating at $TE_{1\delta 1}$ and $TE_{1\delta 3}$ modes can be differentially fed by the coplanar strip line (CPS) and then is used as a driver, which functions as a dual-mode magnetic dipole (M-dipole) resulting from the $TE_{1\delta 1}$ and $TE_{1\delta 3}$ modes. Thus, a dual-band quasi-Yagi antenna with two close operation frequencies can be designed, meanwhile, the two bands can be independently controlled. Based on this, a wide-band quasi-Yagi antenna is introduced by adding two metal directors with different sizes on the top and bottom layers of the supporting substrate. The two directors provide two additional resonant frequencies, turning dual-band antenna into a wide-band one. To verify the design concepts, two prototypes of dual- and wide-band antennas are fabricated and measured. Good agreement between the simulated and measured results can be observed. The wide-band antenna has a measured -10 dB impedance bandwidth of 21.7 % (9.33 - 11.6 GHz). Within it, the peak gain of antenna is 8 dBi and 1 dB gain bandwidth is 15.5%.

INDEX TERMS Quasi-Yagi antenna, dielectric resonator (DR), M-dipole, dual-band, wide-band, high gain.

I. INTRODUCTION

With the development of wireless systems, endfire antennas have drawn extensive attention due to their specific applications, such as point-to-point communication systems and radar imaging systems. Up to now, different types of endfire antenna are studied and developed worldwide, including log-periodic antennas, horn antennas, surface-wave antennas, and quasi-Yagi antennas. The log-periodic antenna has ultrawide bandwidth for endfire radiation, but its endfire gain is limited due to the partly radiated property [1]. The traditional metallic horn antenna has high gain and wide bandwidth, but is large in size and heavy in weight. To reduce the weight of the horn antenna, substrate integrated waveguide (SIW) horn antenna is presented. However, on account of its thin open end, it has narrow operating band [2]. The Vivaldi antenna also has characteristic of broadband, but the cross-polarization and side lobes will deteriorate rapidly as the operating frequency increases [3]. The quasi-Yagi antenna, a typical type of parasitic element antenna, has lots of advantages, such as simple

The associate editor coordinating the review of this manuscript and approving it for publication was Mohammed Bait-Suwailam¹.

structure, light weight, high directivity and easy forming array, which make it attractive [4]–[9].

The traditional quasi-Yagi antenna has narrow operating band generally [10]–[12], which could not meet the multi-frequency operation requirements of modern wireless communication. Accordingly, lots of dual-band and wide-band quasi-Yagi antennas are reported. Among them, electric dipole (E-dipole) and magnetic dipole (M-dipole) are commonly used [13]–[21]. There are two common methods to obtain dual-band operation. One is utilizing double E-dipoles [13]–[16]. However, this method will enlarge the longitudinal size of the radiating element and limit the gain. The other is adding parasitic components [17]–[20]. Since this method requires the parasitic elements to be placed very close to the driver, the gain will be negatively affected. For wide-band designs, employing multi E-/M-dipoles and parasitic components are still effective methods [21]–[24]. What's more, improving impedance matching can also enhance the bandwidth. In [25], a bowtie driver is adopted to improve the impedance matching. In [26] and [27], to enlarge operating band, wideband feeding structures are developed. However, this method can only enlarge impedance bandwidth while gain fluctuates greatly in low frequency range of the

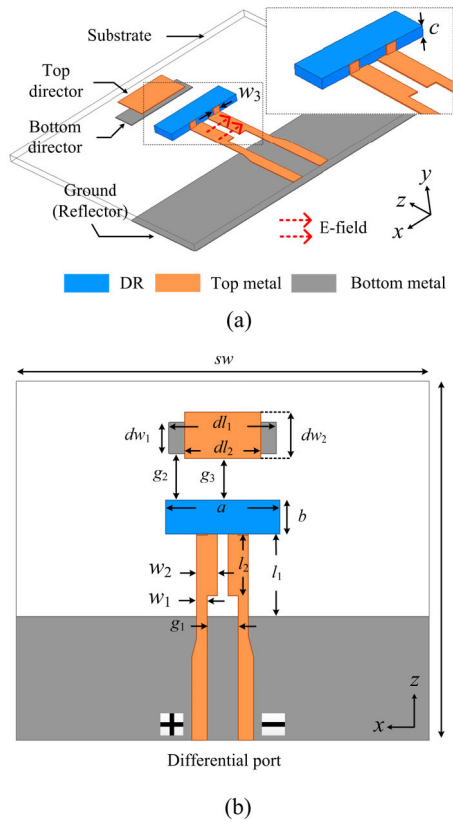


FIGURE 1. Configuration of proposed wide-band quasi-Yagi antenna with directors, (a) 3-D view, (b) top view. ($sl = 34$ mm, $sw = 30$ mm, $l_1 = 8$ mm, $l_2 = 6$ mm, $g_1 = 1.5$ mm, $g_2 = 3.5$ mm, $g_3 = 3$ mm, $dl_1 = 7.8$ mm, $dw_1 = 2.8$ mm, $dl_2 = 7.8$ mm, and $dw_2 = 4$ mm, $w_1 = 1$ mm, $w_2 = 1.6$ mm, and $w_3 = 1$ mm).

operating band. This is due to the limitation of driver’s bandwidth with good radiation. As given in [26], the design has 75% impedance fractional bandwidth (FBW). Within it, gain ranges from 4 dBi to 8 dBi and 1 dB gain FBW is only 2%.

It is well known that dielectric resonator (DR) has several advantages, such as high radiation efficiency and flexible design, and then is extensively applied in wireless communication systems [28]–[31]. In [32], a quasi-Yagi antenna based on a DR is reported, which has higher gain over traditional metal quasi-Yagi antenna. However, it has a narrow FBW of 3% because only one $TE_{1\delta 1}$ mode is used. In this paper, a dual-/wide-band quasi-Yagi antenna using a rectangular DR driver is presented. The $TE_{1\delta 1}$ and $TE_{1\delta 3}$ modes of the DR are simultaneously excited and used as for designing dual-band antenna. Furthermore, by introducing two directors in front of the DR driver for generating two additional resonant frequencies between the two modes, a wide-band quasi-Yagi antenna comes into being. Meanwhile, the antenna gain can also be enhanced by the directors.

II. ANTENNA DESIGN

A. DR ANALYSIS

The configuration of the proposed quasi-Yagi antenna is shown in Fig. 1. A rectangular DR ($a \times b \times c$) is put on the top

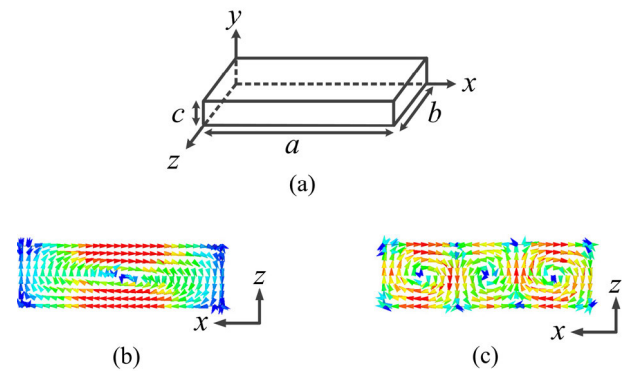


FIGURE 2. Rectangular DR, (a) 3-D view, (b) E-field of $TE_{1\delta 1}$ mode, (c) E-field of $TE_{1\delta 3}$ mode.

of a substrate ($sl \times sw$). The DR is made of ceramic material ($\epsilon_{r1} = 69$ and $\tan\delta = 0.0085$), whose chemical composition is $Ba_2Sm_7Ti_9O_{26}$ and the manufacturer of ceramics is Jiangsu Jiangjia Electronic Co., Ltd, China. The substrate is Rogers 4003C laminate with a dielectric constant of $\epsilon_{r2} = 3.38$ and a loss tangent of $\tan\delta = 0.0027$. The DR is differentially fed through a balanced transmission line, i.e. coplanar strip line (CPS) on the top of substrate. The ground plane on the bottom of the substrate is used as a reflector for achieving an end-fire radiation. There are two metal directors, i.e. bottom director ($dl_1 \times dw_1$) and top director ($dl_2 \times dw_2$), in front of the DR driver.

Fig. 2(a) shows a 3-D rectangular DR, and its resonant frequency (f_R) of $TE_{m\delta n}$ modes can be calculated by (1) below [33].

$$\begin{cases} k_x^2 + k_y^2 + k_z^2 = \epsilon_r k_0^2 \\ k_y \tan\left(\frac{k_y c}{2}\right) = \sqrt{(\epsilon_r - 1)k_0^2 - k_x^2} \\ k_x = \frac{m\pi}{a}, k_y = \frac{\delta\pi}{c}, k_z = \frac{n\pi}{b} \\ f_R = \frac{c_v k_0}{2\pi} \end{cases} \quad (1)$$

where $k_x = m\pi/a$ and $k_z = n\pi/b$ are the wavenumbers along the x - and z -directions respectively, m and n denotes the number of field extrema in the x - and z -direction, c_v is the speed of light in vacuum, k_0 is the free-space wave number.

The E-field distributions of the $TE_{1\delta 1}$ and $TE_{1\delta 3}$ modes are shown in Fig. 2(b) and (c), which circulate azimuthally and are tangential to the x - z plane. Thus, both $TE_{1\delta 1}$ and $TE_{1\delta 3}$ modes of rectangular DR can be regarded as a dual-mode M-dipole in y -direction, which can be equivalent to a dual-mode E-dipole in x -direction [33]. In Fig. 3, the calculated and simulated resonance frequencies of $TE_{1\delta 1}$ and $TE_{1\delta 3}$ are very consistent, which means that the design can be guided through the formulas. Besides, in order to maintain the low profile and save the area of the xoz plane of the DR resonator in this design, the height c of the DR resonator is set as $c = 1$ mm in y -direction and the dielectric constant ϵ_r is 69. When c and ϵ_r are fixed, according to resonance frequency,

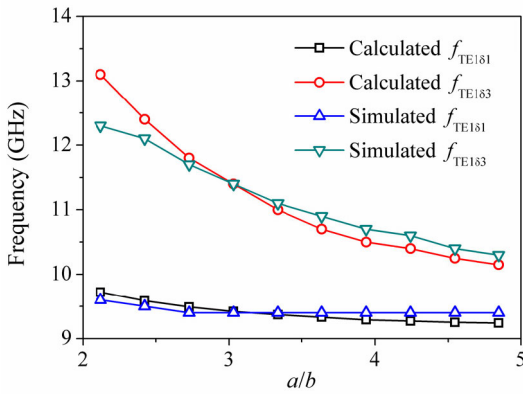


FIGURE 3. The curve of frequencies of the TE_{1δ1} and TE_{1δ3} modes under different a/b . ($b = 3.3$ mm, $c = 1$ mm and $\epsilon_{r1} = 69$ are fixed).

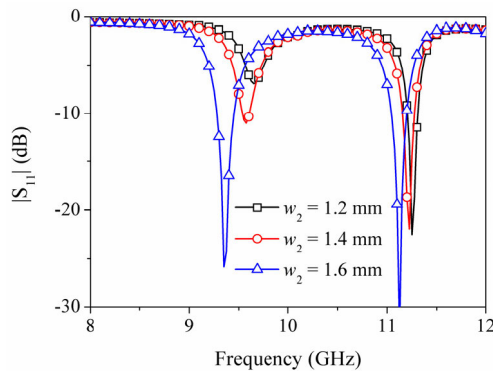


FIGURE 4. Simulated $|S_{11}|$ under different w_2 .

length a and width b can be decided. As can be seen from Fig. 3, when a/b is more than 3, the frequency of TE_{1δ3} can be shifted down and is close to that of TE_{1δ1} mode since the TE_{1δ1} mode varies slightly. To design an X-band dual-band quasi-Yagi antenna with a lower band at about 9.5GHz (TE_{1δ1} mode), Thus, $a = 11.5$ mm, $b = 3.3$ mm, $c = 1$ mm and $\epsilon_{r1} = 69$ are chosen.

B. DUAL-BAND ANTENNA

Based on the above mode analysis, the rectangular DR can be used as a dual-mode M-dipole operating at two close frequencies. Accordingly, a dual-band quasi-Yagi antenna can be designed by differentially exciting the TE_{1δ1} and TE_{1δ3} modes, where the directors shown in Fig. 1 are not included here. As shown in Fig. 2 (b) and (c), there is an E-field circle inside of the DR for the TE_{1δ1} mode while three E-field circles for the TE_{1δ3} modes. To excite the two modes simultaneously, the feeding points of differential line pair of the CPS on the DR should locate in the vicinity of the DR center so that the E-field distribution of the CPS is consistent with those of the two modes. Under this condition, the stepped-width CPS is adopted to achieve good impedance matching in the dual-band of the proposed antenna simultaneously. As shown in Fig. 4, with w_2 increasing, $|S_{11}|$ is improved. Tuning l_2

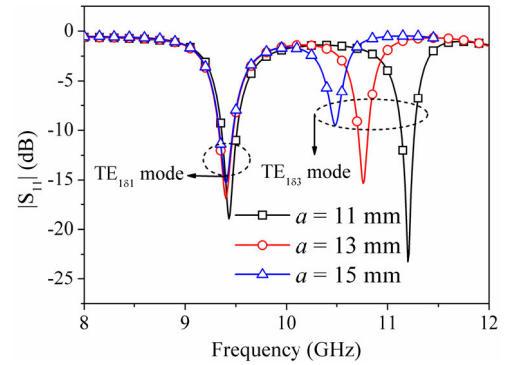


FIGURE 5. Simulated $|S_{11}|$ of proposed dual-band antenna without directors under different a .

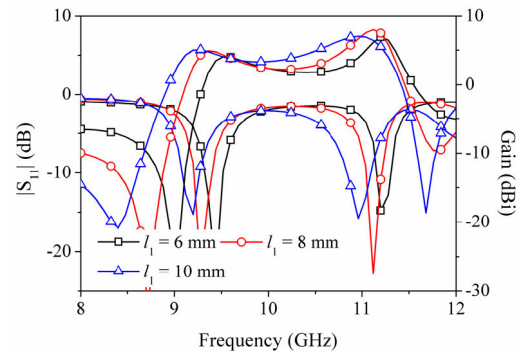


FIGURE 6. The curve of frequencies of the TE_{1δ1} and TE_{1δ3} modes under different a/b . ($b = 3.3$ mm, $c = 1$ mm and $\epsilon_{r1} = 69$ are fixed).

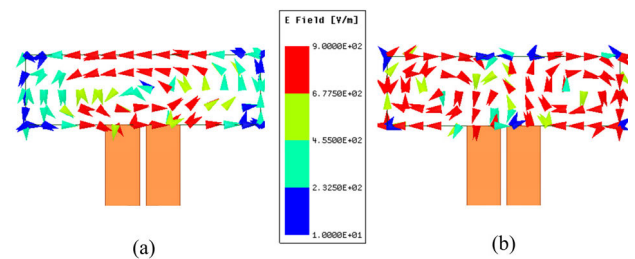


FIGURE 7. E-field of proposed antenna without directors, (a) in lower band, (b) in upper band.

can have the same effect. Fig. 5 shows the simulated $|S_{11}|$ under different a . As expected, the upper band resulting from TE_{1δ3} mode of the DR can be independently tuned while the lower band from TE_{1δ1} mode remains unchanged almost. The distance between ground and DR driver is noted as l_1 , as shown in Fig. 1. In Fig. 6, with different l_1 , the peak gain of lower and upper band is affected. According to this result, $l_1 = 8$ mm is chosen for balance. The E-field of lower and upper bands of proposed dual-band antenna are presented in Fig. 7 (a) and (b), corresponding to the TE_{1δ1} mode and TE_{1δ3} mode of the DR, respectively, as can be seen from Fig. 2(b) and 2(c). Besides, the transverse width sw of the ground reflector also has evident effect on the dual-band gains, as shown in Fig. 8. As sw increases, the gains of both bands are improved.

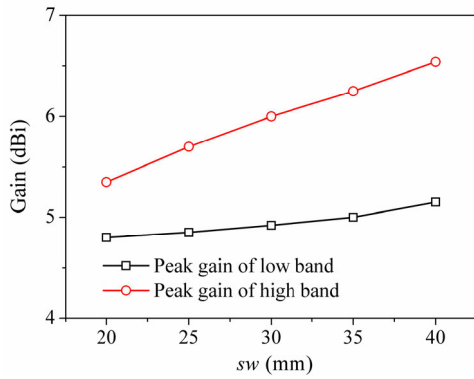


FIGURE 8. Simulated peak gain of proposed dual-band antenna without directors against the reflector width sw .

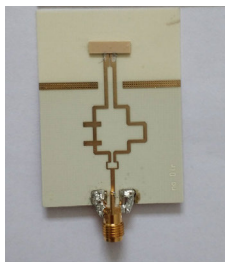


FIGURE 9. Photograph of the fabricated dual-band antenna. ($sl = 34$ mm, $sw = 30$ mm, $l_1 = 8$ mm, $l_2 = 3.8$ mm, $g_1 = 1.5$ mm, $w_1 = 1$ mm, $w_2 = 1.6$ mm, and $w_3 = 1$ mm).

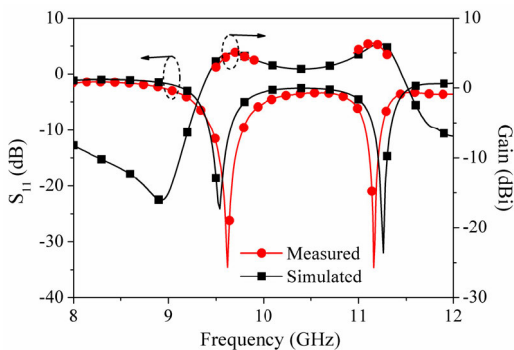


FIGURE 10. The simulated and measured $|S_{11}|$ and gain of the proposed dual-band antenna.

The photograph and dimensions of the proposed dual-band antenna are presented in Fig. 9. A microstrip wide-band balun is designed to connect with the CPS for antenna test [34]. Fig. 10 shows the simulated and measured $|S_{11}|$ and gain of proposed dual-band antenna. The measured FBWs ($|S_{11}| < -10$ dB) of the lower and upper bands are about 3% (9.46 - 9.78 GHz) and 1.7% (11.01 - 11.25 GHz) respectively. In the lower and upper bands, the peak gains are 5.1 dBi and 6.4 dBi, respectively.

Fig. 11 depicts the simulated and measured radiation patterns in both E- and H-planes at 9.62 GHz and 11.15 GHz. The cross-polarization levels of less than -18 dB are observed within $\pm 30^\circ$ beam width.

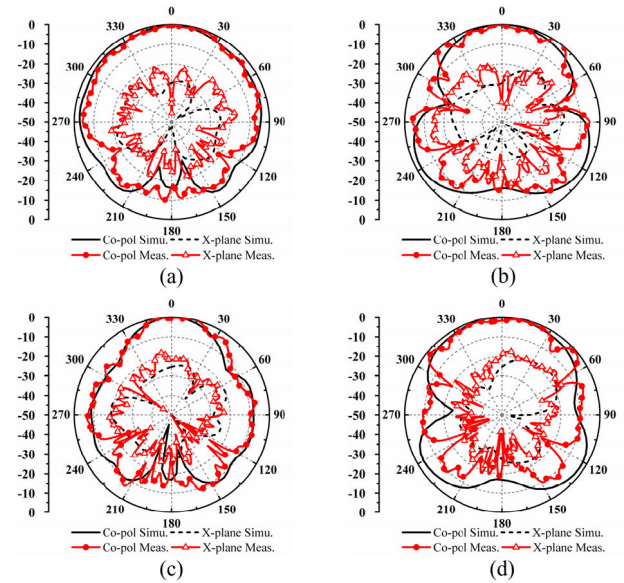


FIGURE 11. The simulated and measured radiation patterns of proposed dual-band antenna, (a) E-plane at 9.62 GHz, (b) H-plane at 9.62 GHz, (c) E-plane at 11.15 GHz, (d) H-plane at 11.15 GHz.

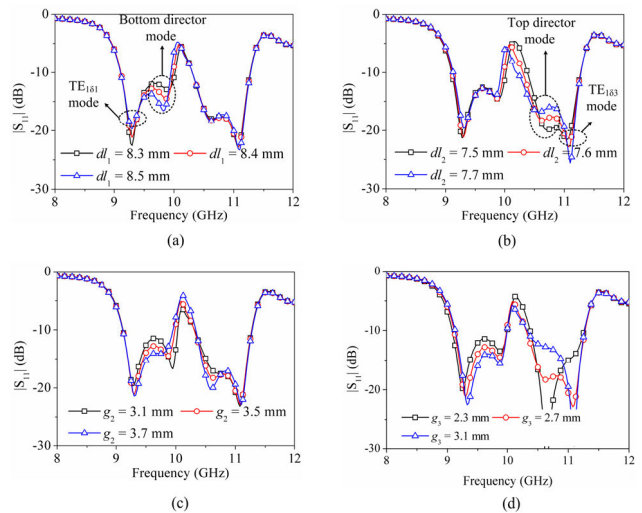


FIGURE 12. Simulated $|S_{11}|$ of proposed Yagi antenna, (a) under different dl_1 , (b) under different dl_2 , (c) under different g_2 , (d) under different dl_2 . ($dl_1 = 8.4$ mm, $dw_1 = 3.0$ mm, $dl_2 = 7.6$ mm, $dw_2 = 3.0$ mm, $g_2 = 3.5$ mm, and $g_3 = 2.5$ mm. Parameter studies only change one parameter while the remaining parameters are fixed).

C. WIDE-BAND ANTENNA

Based on the dual-band design, a wide-band design is introduced by adding two metal directors with different sizes on the top and bottom layers, as shown in Fig. 1. Since the directors are placed near the driver, the directors can be excited by the DR driver to provide additional resonant frequencies [35]. The long director with a length dl_1 on the bottom of the substrate is used to generate a resonance near to the TE_{181} mode of the DR while the short director a length dl_2 on the top of the substrate is used to generate a resonance near to the TE_{183} mode of the DR, as shown in Fig. 12. These two

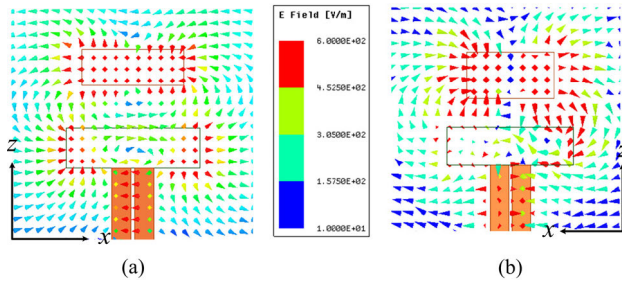


FIGURE 13. E-field of proposed antenna with directors, (a) resonance of bottom director, (b) resonance of top director.

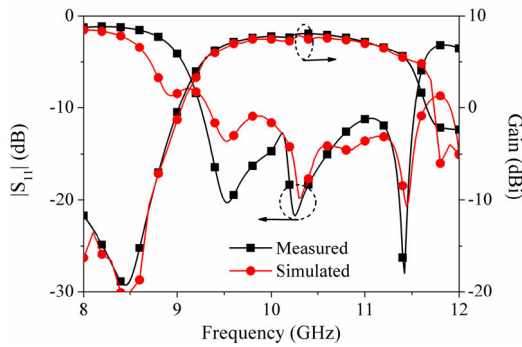


FIGURE 14. The simulated and measured $|S_{11}|$ and gain of the proposed wide-band antenna.

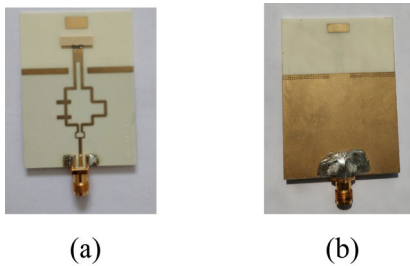


FIGURE 15. Photograph of the proposed wide-band antenna, (a) top view, (b) bottom view (The dimensions are available in Fig. 1).

resonance points generated by the directors can also be fine-tuned by adjusting distance between them and DR, which can be seen from Fig. 12 (c) and (d). The E-field of resonance points of directors have been presented in Fig. 13. Fig. 13 (a) shows the E-field of resonance point of bottom director (long director). It can be found that the strength of E-field in bottom director is considerable. Similarly, Fig. 13 (b) shows the E-field of resonance point of top director (short director) and the strength is also remarkable.

By optimizing the parameters of the directors and director locations (represented by the distances g_2 and g_3 between the DR driver and bottom and top directors), a wide-band response can be obtained, as shown in Fig. 14.

III. WIDE-BAND ANTENNA RESULTS AND DISCUION

To verify this idea, the proposed wide-band antenna is designed and fabricated. Similarly, a microstrip wide-band

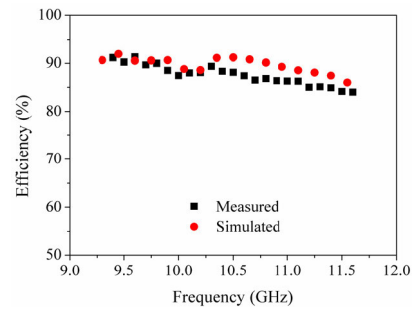


FIGURE 16. Measured and simulated radiation efficiency of the proposed antenna.

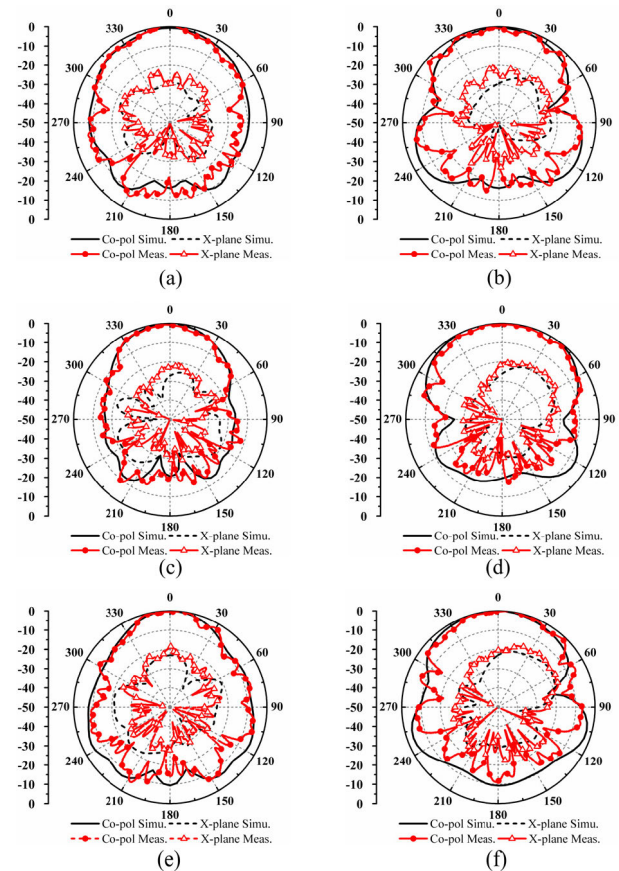


FIGURE 17. The simulated and measured radiation patterns of proposed wide-band antenna (a) E-plane at 9.48 GHz, (b) H-plane at 9.48 GHz, (c) E-plane at 10.34 GHz, (d) H-plane at 10.34 GHz, (e) E-plane at 11.42 GHz, (f) H-plane at 11.42 GHz.

balun is designed to connect with the CPS for antenna test. Fig. 15 shows the photographs of the implemented antenna with directors. In Fig. 14, the simulated and measured $|S_{11}|$ and gain of proposed antenna are presented. The measured impedance FBW ($|S_{11}| < -10$ dB) is about 21.7% from 9.33 to 11.6 GHz. Within it, the measured peak gain is 8 dBi, and 1dB gain FBW is about 15.5% from 9.5 to 11.1 GHz. The radiation efficiency of proposed wide-band quasi-Yagi antenna is presented in Fig. 16. In the operating band, the measured radiation efficiency is from 85% to 92%. Fig. 17 shows the simulated and measured radiation

TABLE 1. Performance comparison with the previous quasi-Yagi antennas.

Ref	Driver Type	N	Peak Gain (dBi)	Impedance FBW(GHz)	1dB Gain FBW(GHz)	Area ($\lambda_0 \times \lambda_0$)
[6]	M-dipole (Microstrip)	3	11	13.1% (4.87-5.55)	6.6% (5.25-5.61)	0.87× 1.9
[23]	M-dipole (Microstrip)	5	11	28.6% (5.0-6.7)	19.8% (5.0-6.1)	1.4× 1.4
[25]	E-dipole (Strip)	4	8	74% (18.6-39.2)	2% (18.0-30.0)	0.84× 0.61
[26]	E-dipole (Strip)	3	6.8	105% (3.6-11.6)	25% (7.8-10.1)	0.36× 0.71
[31]	M-dipole (DR)	2	8.4	3% (8.97-9.27)	3% (8.97-9.27)	0.85× 1.3
This work	M-dipole (DR)	3	8	21.7% (9.33-11.6)	15.5% (9.5-11.1)	0.60× 1.05

λ_0 means the free-space wavelength at the center frequency of the impedance bandwidth.

N means number of drivers and directors.

patterns in both E- and H-planes at 9.52 GHz, 10.34 GHz, and 11.42 GHz, respectively. The cross-polarization levels of less than -16 dB are observed within $\pm 30^\circ$ beam width. As can be seen from Fig. 14, Fig. 16, and Fig. 17, little disparity can be observed between the simulated and measured results, which can be attributed to the error of fabrication and implementation.

The comparison of the proposed antenna with previous quasi-Yagi antennas is summarized in Table 1. In [6], a microstrip M-dipole quasi-Yagi antenna is reported. Although it has high gain, its transverse size is close to $2\lambda_0$ and its 1 dB gain FBW is only 6.6%. In [24], five microstrip magnetic dipoles with series feeding structure are employed to enhance bandwidth, and the bandwidth is about 28.6% and the gain is about 10dBi in the operating band. However this structure brings large longitudinal length and it is a challenging working to achieve further gain due to the difficulty in adding proper directors. Moreover, the transverse length of magnetic dipole driver is about one λ_0 . In the proposed design, the transverse length of the DR driver is about $0.3\lambda_0$ and the transverse size of whole antenna ground is only about one λ_0 . In [26] and [27], both of them have more than 70% impedance FBW, but the gain levels are not good. In [32], an M-dipole quasi-Yagi antenna based on a DR is introduced. Since only dominant $TE_{1\delta 1}$ mode is employed, the impedance FBW of operating band is only 3%.

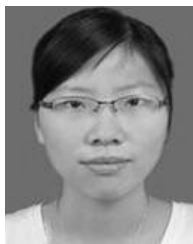
IV. CONCLUSION

In this paper, a dual-/wide-band quasi-Yagi antenna using a DR has been presented. The $TE_{1\delta 1}$ and $TE_{1\delta 3}$ modes of the DR can be effectively excited at the same time and used as a dual-mode dipole for designing a dual-band Yagi antenna. By introducing two metal directors with different sizes in front of DR driver, the dual-band antenna can be effectively transformed to a wideband one. The demonstration antennas have been designed and implemented, and the simulated and measured results with good accordance have been presented.

REFERENCES

- [1] D. Isbell, "Log periodic dipole arrays," *IRE Trans. Antennas Propag.*, vol. 8, no. 3, pp. 260–267, May 1960.
- [2] L. Sun, B. Sun, J. Yuan, W. Tang, and H. Wu, "Low-profile, quasi-omnidirectional substrate integrated waveguide (SIW) multihorn antenna," *IEEE Antennas Wireless Propag. Lett.*, vol. 15, pp. 818–821, 2016.
- [3] J. Puskely, J. Lacik, Z. Raida, and H. Arthaber, "High-gain dielectric-loaded Vivaldi antenna for Ka-band applications," *IEEE Antennas Wireless Propag. Lett.*, vol. 15, pp. 2004–2007, 2016.
- [4] G. Liu, Y. M. Pan, T. L. Wu, and P. F. Hu, "A compact planar quasi-Yagi antenna with bandpass filtering response," *IEEE Access*, vol. 7, pp. 67856–67862, 2019.
- [5] B. S. Abirami and E. F. Sundarsingh, "EBG-backed flexible printed Yagi-Uda antenna for on-body communication," *IEEE Trans. Antennas Propag.*, vol. 65, no. 7, pp. 3762–3765 Jul. 2017.
- [6] J. H. Liu and Q. Xue, "Microstrip magnetic dipole Yagi array antenna with endfire radiation and vertical polarization," *IEEE Trans. Antennas Propag.*, vol. 61, no. 3, pp. 1140–1147, Mar. 2013.
- [7] F. Wei, X. B. Zhao, and X. W. Shi, "A balanced filtering quasi-Yagi antenna with low cross-polarization levels and high common-mode suppression," *IEEE Access*, vol. 7, pp. 100113–100119, 2019.
- [8] A. Abbosh, "Ultra-wideband quasi-Yagi antenna using dual-resonant driver and integrated balun of stepped impedance coupled structure," *IEEE Trans. Antennas Propag.*, vol. 61, no. 7, pp. 3885–3888, Jul. 2013.
- [9] E. Guo, J. Liu, and Y. Long, "A mode-superposed microstrip patch antenna and its Yagi array with high front-to-back ratio," *IEEE Trans. Antennas Propag.*, vol. 65, no. 12, pp. 7328–7333, Dec. 2017.
- [10] Y. Luo and Q. X. Chu, "A Yagi-Uda antenna with a stepped-width reflector shorter than the driven element," *IEEE Antennas Wireless Propag. Lett.*, vol. 15, pp. 564–567, 2016.
- [11] L. Qun, R. X. Wu, and Y. B. Tian, "A rectangular loop Yagi-Uda antenna by the two materials 3-D printing technology," *IEEE Antennas Wireless Propag. Lett.*, vol. 17, no. 11, pp. 2017–2020, Nov. 2018.
- [12] G. R. Dejean and M. M. Tentzeris, "A new high-gain microstrip Yagi array antenna with a high front-to-back (F/B) ratio for WLAN and millimeter-wave applications," *IEEE Trans. Antennas Propag.*, vol. 55, no. 2, pp. 298–304, Feb. 2007.
- [13] S. A. Alekseytsev and A. P. Gorbachev, "The novel printed dual-band quasi-Yagi antenna with ends-fed dipole-like driver," *IEEE Trans. Antennas Propag.*, to be published.
- [14] H.-C. Huang, J.-C. Lu, and P. Hsu, "A compact dual-band printed Yagi-Uda antenna for GNSS and CMMB applications," *IEEE Trans. Antennas Propag.*, vol. 63, no. 5, pp. 2342–2348, May 2015.
- [15] K. D. Xu, D. Li, Y. Liu, and Q. H. Liu, "Printed quasi-Yagi antennas using double dipoles and stub-loaded technique for multi-band and broadband applications," *IEEE Access*, vol. 6, pp. 31695–31702, 2018.
- [16] J. Yeo and J.-I. Lee, "Bandwidth enhancement of double-dipole quasi-Yagi antenna using stepped slotline structure," *IEEE Antennas Wireless Propag. Lett.*, vol. 15, pp. 694–697, 2016.
- [17] D. O. Kim and C. Y. Kim, "Dual-band quasi-Yagi antenna with split ring resonator directors," *Electron. Lett.*, vol. 48, no. 14, pp. 809–810, Jul. 2012.
- [18] Z. Hu, Z. Shen, W. Wu, and J. Lu, "Low-profile top-hat monopole Yagi antenna for end-fire radiation," *IEEE Trans. Antennas Propag.*, vol. 63, no. 7, pp. 2851–2857, Jul. 2015.
- [19] S. S. Jehangir and M. S. Sharawi, "A miniaturized UWB biplanar Yagi-like MIMO antenna system," *IEEE Antennas Wireless Propag. Lett.*, vol. 16, pp. 2320–2323, 2017.
- [20] S. S. Jehangir, M. S. Sharawi, and A. Shamim, "Highly miniaturized semi-loop meandered dual-band MIMO antenna system," *IET Microw. Antennas Propag.*, vol. 12, no. 6, pp. 864–871, May 2018.
- [21] B.-K. Tan, S. Withington, and G. Yassin, "A compact microstrip-fed planar dual-dipole antenna for broadband applications," *IEEE Antennas Wireless Propag. Lett.*, vol. 15, pp. 593–596, 2016.
- [22] S. Ahdi Rezaeieh, M. A. Antoniadis, and A. M. Abbosh, "Miniaturization of planar Yagi antennas using mu-negative metamaterial-loaded reflector," *IEEE Trans. Antennas Propag.*, vol. 65, no. 12, pp. 6827–6837, Dec. 2017.
- [23] S.-W. Qu, J.-L. Li, Q. Xue, and C.-H. Chan, "Wideband periodic endfire antenna with bowtie dipoles," *IEEE Antennas Wireless Propag. Lett.*, vol. 7, pp. 314–317, 2008.
- [24] L. Yang, W. Wu, and J.-D. Zhang, "Wideband microstrip series-fed magnetic dipole array antenna," *Electron. Lett.*, vol. 50, no. 24, pp. 1793–1795, Nov. 2014.

- [25] S. A. Rezaeieh, M. A. Antoniadis, and A. M. Abbosh, "Miniaturized planar Yagi antenna utilizing capacitively coupled folded reflector," *IEEE Antennas Wireless Propag. Lett.*, vol. 16, pp. 1977–1980, 2017.
- [26] H. Chu, Y.-X. Guo, H. Wong, and X. Shi, "Wideband self-complementary quasi-Yagi antenna for millimeter-wave systems," *IEEE Antennas Wireless Propag. Lett.*, vol. 10, pp. 322–325, 2011.
- [27] J. Wu, Z. Zhao, Z. Nie, and Q.-H. Liu, "Bandwidth enhancement of a planar printed quasi-Yagi antenna with size reduction," *IEEE Trans. Antennas Propag.*, vol. 62, no. 1, pp. 463–467, Jan. 2014.
- [28] Y. M. Pan and S. Y. Zheng, "A low-profile stacked dielectric resonator antenna with high-gain and wide bandwidth," *IEEE Antennas Wireless Propag. Lett.*, vol. 15, pp. 68–71, 2016.
- [29] W.-W. Yang, X.-Y. Dong, W.-J. Sun, and J.-X. Chen, "Polarization reconfigurable broadband dielectric resonator antenna with a lattice structure," *IEEE Access*, vol. 6, pp. 21212–21219, 2018.
- [30] U. Illahi, J. Iqbal, M. I. Sulaiman, M. M. Alam, M. M. Su'ud, and M. H. Jamaluddin, "Singly-fed rectangular dielectric resonator antenna with a wide circular polarization bandwidth and beamwidth for WiMAX/Satellite applications," *IEEE Access*, vol. 7, pp. 66206–66214, 2019.
- [31] P. F. Hu, Y. M. Pan, K. W. Leung, and X. Y. Zhang, "Wide-/dual-band omnidirectional filtering dielectric resonator antennas," *IEEE Trans. Antennas Propag.*, vol. 66, no. 5, pp. 2622–2627, May 2018.
- [32] Z. Y. Qian, W. J. Sun, X. F. Zhang, and J. X. Chen, "An X-band magnetic dipole quasi-Yagi antenna based on a dielectric resonator," *Int. J. Microw. Wireless Technol.*, to be published.
- [33] K. M. Luk, and K. W. Leung, *Dielectric Resonator Antennas*. Baldock, U.K.: Research Studies, 2003.
- [34] Z.-Y. Zhang, Y.-X. Guo, L. Chuen Ong, and M. Chia, "A new wide-band planar balun on a single-layer PCB," *IEEE Microw. Wireless Compon. Lett.*, vol. 15, no. 6, pp. 416–418, Jun. 2005.
- [35] H. Xu, Y. Li, D. Ye, and Y. Long, "A broadband offset-parallel-parallelgrams printed endfire antenna," *IEEE Antennas Wireless Propag. Lett.*, vol. 16, pp. 1167–1170, 2017.



LING-LING YANG was born in Nantong, Jiangsu, China, in 1987. She received the B.Sc. degree in electronic science and technology from Xinglin College, Nantong University, Nantong, in 2009, and the M.Sc. degree in information and communication engineering from Nantong University, in 2012. Since 2012, she has been with Xinglin College, Nantong University, where she is currently a Lecturer. Her current research interest includes dielectric resonator antenna.



JIAN-XIN CHEN (Senior Member, IEEE) was born in Nantong, Jiangsu, China, in 1979. He received the B.S. degree from Huai Yin Teachers College, Jiangsu, in 2001, the M.S. degree from the University of Electronic Science and Technology of China (UESTC), Chengdu, China, in 2004, and the Ph.D. degree from the City University of Hong Kong, Kowloon, Hong Kong, in 2008. Since 2009, he has been with Nantong University, Jiangsu, where he is currently a Professor. He has

authored or coauthored more than 80 internationally referred journal and conference papers. He holds three Chinese patents and two U.S. patents. His research interests include microwave active/passive circuits and antennas and LTCC-based millimeter-wave circuits and antennas.

Dr. Chen was a recipient of the Best Paper Award presented at the Chinese National Microwave and Millimeter-Wave Symposium, Ningbo, China, in 2007. He was a Supervisor of the 2014 iWEM Student Innovation Competition Winner in Sapporo, Japan.

• • •



ZHONG-YU QIAN was born in Siyang, Jiangsu, China, in 1994. He received the B.Sc. degree in electronic science and technology from Nantong University, Nantong, China, in 2016, where he is currently pursuing the M.Sc. degree in electromagnetic field and microwave technology. His current research interests include filter and antenna.